

1 **Contact tracing efficiency, transmission heterogeneity, and accelerating COVID-**  
2 **19 epidemics**

3

4 Billy J. Gardner, A. Marm Kilpatrick\*

5

6 *Department of Ecology and Evolutionary Biology, University of California, Santa Cruz*

7 *\*Correspondence to [akilpatr@ucsc.edu](mailto:akilpatr@ucsc.edu)*

8

9

10 **Abstract**

11 Simultaneously controlling COVID-19 epidemics and limiting economic and societal  
12 impacts presents a difficult challenge, especially with limited public health budgets.  
13 Testing, contact tracing, and isolating/quarantining is a key strategy that has been used  
14 to reduce transmission of SARS-CoV-2, the virus that causes COVID-19. However,  
15 manual contact tracing is a time-consuming process and as case numbers increase it  
16 takes longer to reach each cases' contacts, leading to additional virus spread. Delays  
17 between symptom onset and being tested (and receiving results), and a low fraction of  
18 symptomatic cases being tested and traced can also reduce the impact of contact  
19 tracing on transmission. We examined the relationship between cases and delays and  
20 the pathogen reproductive number  $R_t$ , and the implications for infection dynamics using  
21 a stochastic compartment model of SARS-CoV-2. We found that  $R_t$  increases  
22 sigmoidally with the number of cases due to decreasing contact tracing efficacy. This  
23 relationship results in accelerating epidemics because  $R_t$  increases, rather than  
24 declines, as infections increase. Shifting contact tracers from locations with high and  
25 low case burdens relative to capacity to locations with intermediate case burdens  
26 maximizes their impact in reducing  $R_t$  (but minimizing total infections is more  
27 complicated). Contact tracing efficacy also decreased with increasing delays between  
28 symptom onset and tracing and with lower fraction of symptomatic infections being  
29 tested. Finally, testing and tracing reductions in  $R_t$  can sometimes greatly delay  
30 epidemics due to the highly heterogeneous transmission dynamics of SARS-CoV-2.  
31 These results demonstrate the importance of having an expandable or mobile team of  
32 contact tracers that can be used to control surges in cases, and the value of easy  
33 access, high testing capacity and rapid turn-around of testing results, as well as  
34 outreach efforts to encourage symptomatic infections to be tested immediately after  
35 symptom onset.

36

## 37 **Author Summary**

38           A key tool in the control of infectious diseases is contact tracing – the  
39 identification of individuals who have contacted the case and may have been infected  
40 by a newly detected case. However, to successfully contact and quarantine individuals  
41 requires time, and as cases rise, this can result in delays in reaching contacts during  
42 which time they may infect other people. Here we examine the quantitative relationships  
43 between increasing case numbers, contact tracing efficiency, and the pathogen  
44 reproductive number  $R_t$  (the number of cases infected by each case) and how these  
45 relationships vary with delays and incomplete participation in the testing and tracing  
46 process. We built

47

## 48 **Introduction**

49           Severe acute respiratory syndrome coronavirus 2 (SARS-CoV-2) emerged in late  
50 2019 spread globally in early 2020 and resulted in rapidly growing local epidemics, large  
51 scale mortality, and strains on hospital capacity in many countries (1-4). Initial outbreaks  
52 in most countries and US states were arrested only by severe control measures  
53 including closing all but essential businesses as well as schools, churches, and other  
54 organizations (5), while a few countries were able to limit transmission, at least  
55 temporarily, primarily with public health measures (6-8). Severe disease control  
56 measures have had devastating impacts on economies and societies (5). Most  
57 countries and US states are now attempting to re-open as many business sectors and  
58 activities as possible while avoiding a rapid rise in infections.

59           Although self-isolation, social distancing, and mask wearing have reduced the  
60 transmission of SARS-CoV-2, additional interventions, including business closures and  
61 working from home, have often been required to keep the pathogen reproductive  
62 number  $R_t$  below 1 (5, 9, 10), especially in the United States. One public health strategy  
63 that has been used effectively to limit transmission in some countries is testing  
64 symptomatic individuals, tracing their contacts to people they may have infected, and  
65 isolating infected individuals and quarantining people that may have become infected  
66 but have yet to show symptoms or test positive for the virus (hereafter abbreviated T-

67 CT-I/Q) (7, 10, 11). If contacts of cases can be found and quarantined or isolated before  
68 or during their infectious period, this can limit onward spread of the virus.

69 Numerous studies have examined the effectiveness and limitations of T-CT-I/Q  
70 on transmission of SARS-CoV-2 (11-18). Many studies have shown that T-CT-I/Q can  
71 substantially reduce the pathogen reproductive ratio,  $R_t$ , but its efficacy depends on the  
72 importance of pre-symptomatic and asymptomatic transmission, delays between  
73 symptom onset and being tested, and the fraction of infections that are tested and  
74 traced (11, 15, 18). Previous studies have explored various parameter values for  
75 contact tracing efficacy by varying the fraction isolated, the fraction symptomatic, and  
76 the contribution to transmission of undetected infections (11, 15, 18). A key unexplored  
77 challenge in implementing T-CT-I/Q is that tracing contacts and ensuring they can  
78 safely quarantine or isolate is a time-consuming process which results in delays  
79 between detecting a case and successfully quarantining their contacts. This delay  
80 reduces the effectiveness of contact tracing as cases increase. Previous studies have  
81 assumed fixed values for contact tracing parameters and thus have not addressed this  
82 issue.

83 Our aim was to examine the relationship between increasing cases, contact  
84 tracing efficacy, and the pathogen reproductive ratio,  $R_t$ , and to examine the potential  
85 outcomes for disease dynamics. We built a compartment model of SARS-CoV-2  
86 transmission, parameterized it with data from the literature, and examined how  $R_t$  varied  
87 with number cases traced, delays between symptom onset and the start of contact  
88 tracing, the numbers of contacts per case, and different fractions of symptomatic cases  
89 being tested and traced. We also simulated a stochastic version of the model with and  
90 without contact tracing to examine how reductions in  $R_t$  affected variation in the timing  
91 of epidemics.

92

## 93 **Methods**

94 We built a susceptible-exposed-infected-recovered (SEIR) compartment model of  
95 SARS-CoV-2 that included four compartments for infected individuals that reflect  
96 symptom severity (asymptomatic,  $I_a$ , pre-symptomatic,  $I_{ps}$ , mildly symptomatic,  $I_{ms}$ , and  
97 severely symptomatic,  $I_{ss}$ ) (Fig S1). The equations of the model are:

$$\begin{aligned}
 &98 \\
 &99 \quad dS/dt = -\kappa\beta S/N(\sigma_a I_a + \sigma_{ps} I_{ps} + \sigma_{ms} I_{ms} + \sigma_{ss} I_{ss}) \\
 &100 \quad dE/dt = \kappa\beta S/N(\sigma_a I_a + \sigma_{ps} I_{ps} + \sigma_{ms} I_{ms} + \sigma_{ss} I_{ss}) - (\varepsilon + q_{E \rightarrow ps} + q_{E \rightarrow a}) E \\
 &101 \quad dI_{ps}/dt = q_{E \rightarrow ps} E - (\varepsilon + q_{ps \rightarrow ms}) I_{ps} \\
 &102 \quad dI_a/dt = q_{E \rightarrow a} E - (\varepsilon + \gamma_a) I_a \\
 &103 \quad dI_{ms}/dt = q_{ps \rightarrow ms} I_{ps} - (\varepsilon + \tau_{ms} + q_{ms \rightarrow ss} + \gamma_{ms}) I_{ms} \quad [\text{eq. 1}] \\
 &104 \quad dI_{ss}/dt = q_{ms \rightarrow ss} I_{ms} - (\varepsilon + \tau_{ss} + \alpha + \gamma_{ss}) I_{ss} \\
 &105 \quad dQ/dt = \varepsilon I_a + \varepsilon I_{ps} + (\varepsilon + \tau_{ms}) I_{ms} + (\varepsilon + \tau_{ss}) I_{ss} - \gamma_Q Q \\
 &106 \quad dR/dt = \gamma_a I_a + \gamma_{ms} I_{ms} + \gamma_{ss} I_{ss} + \gamma_Q Q
 \end{aligned}$$

107  
 108 where  $\kappa$  is a social distancing factor between 0 and 1 that scales the contact rate  $\beta$ ,  $\sigma$   
 109 are relative infectiousness values for each of the I classes,  $q$  are transition rates  
 110 between classes given by the subscripts separated by the arrow ( $q_{E \rightarrow ps}$  is the transition  
 111 rate between the E and  $I_{ps}$  classes),  $\varepsilon$  is the rate of removal by contact tracing from the  
 112 E or I classes to the quarantined class Q,  $\tau$  are the removal rate by testing of mildly  
 113 symptomatic or severely symptomatic infected individuals,  $\alpha$  is the disease-caused  
 114 death rate, and  $\gamma$  are the recovery rates to the R class.

115 The contact tracing removal rate  $\varepsilon$  is given by:

$$116 \quad \varepsilon = \frac{f_{SCT} q_{E \rightarrow ps}}{q_{E \rightarrow ps} + q_{E \rightarrow a}} \frac{1}{1/\tau_{ms} + 0.5 \frac{I_{ps} q_{ps \rightarrow ms} N_{CPC}}{N_{CT} N_{CCTD}}} \quad [\text{eq. 2}]$$

117 The first term is the fraction of infections traced;  $f_{SCT}$  is the fraction of symptomatic  
 118 infections that are traced of those detected with test removal rate  $\tau_{ms}$  before they  
 119 recover or progress to severe symptoms;  $f_{SCT}$  is equal to  $f_{tmstr} * \tau_{ms} / (\tau_{ms} + q_{ms \rightarrow ss} + \gamma_{ms})$ ;  $f_{SCT}$   
 120 is multiplied by the ratio of transition rates [ $q_{E \rightarrow ps} / (q_{E \rightarrow ps} + q_{E \rightarrow a})$ ] which is the fraction of  
 121 infections that are symptomatic;  $f_{tmstr}$  is the fraction of mildly symptomatic cases  
 122 detected by testing that were traced. We didn't include tracing from severely  
 123 symptomatic cases because, by the time an infection progresses to severe symptoms  
 124 5-8 days after symptom onset (19, 20), their contacts will already have finished most of  
 125 their infectious period, and quarantining their contacts will have little effect.

126 The second term is the inverse of the time between symptom onset of the

127 symptomatic infection and being removed by contact tracing which is the sum of the  
128 delay between symptom onset and receiving a test result,  $1/\tau_{ms}$ , and the average time  
129 needed to reach the contacts of the newly detected cases (which is half the total time to  
130 call all contacts).  $q_{ps \rightarrow ms} I_{ps}$  is the rate of new symptomatic infections that need to be  
131 traced,  $N_{cpc}$  is the average number of contacts per case,  $N_{CT}$  is the number of contact  
132 tracers, and  $N_{CCTD}$  is the number of calls each contact tracer can make each day.

133 We parameterized the model with data from the literature, with all rates in days<sup>-1</sup>  
134 (Table 1) and used the baseline contact tracing capacity standards suggested by the  
135 US National Association of County and City Health Officials (15 contact tracers per  
136 100,000 people; <https://www.naccho.org/uploads/full-width-images/Contact-Tracing-Statement-4-16-2020.pdf>). We note that while notifying individuals that they have had  
138 contact with a case can be done quickly (especially with using a cell-phone tracing app;  
139 (18)), successfully ensuring a contact has their needs met (including food, medicine,  
140 clothing) to quarantine in a safe space where they won't infect their household members  
141 requires substantially more time (<https://www.cdc.gov/coronavirus/2019-ncov/php/notification-of-exposure.html>). We assumed the approximate duration required  
142 for a successful contact tracing call was 40 min, resulting in  $N_{CCTD} = 12$

144 We used the next generation matrix technique to derive an expression for the  
145 pathogen reproductive ratio  $R_t$  (21):

146

147  $R_t = S/N[\kappa\beta]^*$

148 
$$\left[ \frac{(q_{E \rightarrow a})(\sigma_a)}{(\varepsilon + \gamma_a)} + \frac{(q_{E \rightarrow ps})(\sigma_{ps})}{(\varepsilon + q_{ps \rightarrow ms})} \right] + \quad [eq. 3]$$

149 
$$\left[ \frac{(q_{E \rightarrow ps})(q_{ps \rightarrow ms})(\sigma_{ms})}{((\varepsilon + q_{ps \rightarrow ms})(\varepsilon + \tau_{ms} + q_{ms \rightarrow ss} + \gamma_{ms}))} \right] +$$

150 
$$\left[ \frac{(q_{E \rightarrow ps})(q_{ps \rightarrow ms})(q_{ms \rightarrow ss})(\sigma_{ss})}{$$

151 
$$((\varepsilon + q_{ps \rightarrow ms})(\varepsilon + \tau_{ms} + q_{ms \rightarrow ss} + \gamma_{ms})(\varepsilon + \tau_{ss} + \alpha + \gamma_{ss}))} \right] ] / (\varepsilon + q_{E \rightarrow a} + q_{E \rightarrow ps})$$

152

153 This expression can be understood as the fraction of the population that is susceptible,  
154  $S/N$  multiplied by the contact rate  $\beta$  (which is scaled by the social distancing factor  $\kappa$ ),  
155 multiplied by the sum of four terms: one for each infected class. Each of the four terms  
156 includes the product of the transition rates  $q$  to reach that class from the E class  
157 multiplied by the infectiousness of that class,  $\sigma$ , divided by the recovery, testing and

158 tracing rates leaving that I class and the I classes before it. Finally, all four terms are  
159 divided by the rates hosts leave the E class which normalizes the rates moving along  
160 each infection pathway.

161 We examined how  $R_t$  and  $R_0$  ( $R_t = R_0$  at beginning of epidemic when  $S \cong N$ )  
162 varied with different numbers of new symptomatic cases detected (a fraction of the  
163 newly symptomatic infection,  $I_{ps} q_{ps \rightarrow ms}$  in eq. 2), delays between symptom onset and the  
164 start of contact tracing ( $1/\tau_{ms}$  in eq. 2), and numbers of contacts per case ( $N_{cpc}$  in eq. 2).  
165 Note that because these three quantities occur as a ratio (with the number of contact  
166 tracers) in equation (2), any combination of values that produce the same number of  
167 case-contacts per contact tracer calls per day will produce the same value of  $R_t$ . We  
168 illustrated the effect of decreasing contact tracing efficiency as infections increased on  
169 disease dynamics and  $R_t$  by simulating a deterministic version of the model in eq. 1 and  
170 plotted  $R_t$  in real time as an epidemic swept through a population over one year. We  
171 also performed a simple sensitivity analysis by determining how much  $R_t$  varied with a  
172 ten percent increase or decrease in each model parameter (Fig S2).

173 Finally, we explored the implications of stochastic variability and contact tracing  
174 on infection dynamics in a scenario roughly based on a moderate size city with partly  
175 effective social distancing. We simulated a stochastic version of the model given by eq  
176 1 where the number of new infections was drawn from a negative binomial distribution  
177 with mean equal to  $R_t$  and dispersion parameter 0.16 which is intermediate between  
178 available estimates for COVID-19 (22-24). We modeled a scenario of a population of  
179 100,000 people where non-pharmaceutical interventions reduced contact rates by 30%  
180 ( $\kappa=0.7$ ) resulting in  $R_0$  with/without contact tracing of 1.32/1.67, testing and contact  
181 tracing took place after an average of  $1/\tau_{ms} = 5$  days after symptom onset, and half of  
182 symptomatic cases detected by testing being traced ( $f_{tmstr} = 0.5$ ). We examined different  
183 initial numbers of latently infected individuals,  $E$ , at the start of the epidemic to  
184 understand how stochastic variation could impact the timing of epidemics when initial  
185 infections were low.

186 R code to reproduce the results is available from:  
187 <https://github.com/marmkilpatrick/Contact-Tracing-Efficiency>

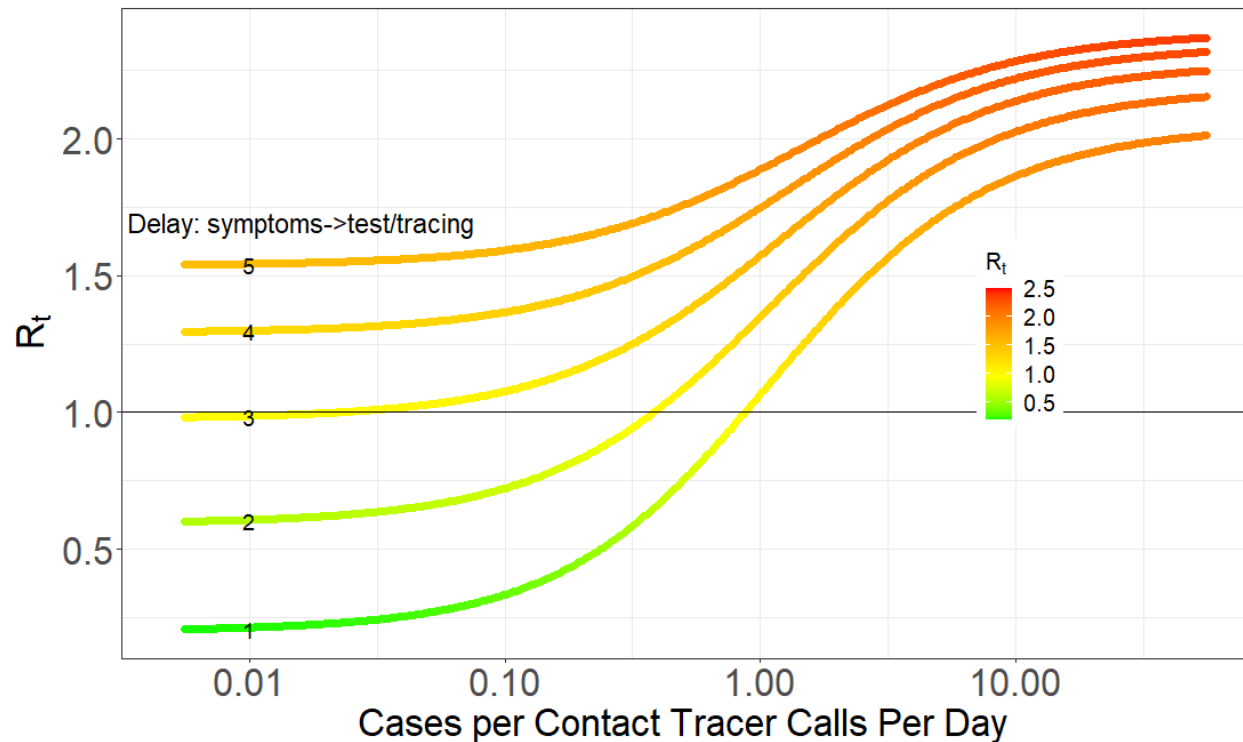
188

189

## 190 Results

191 The effectiveness of contact tracing in reducing the pathogen reproductive  
192 number,  $R_t$ , was highly dependent on three factors: the number of cases being traced  
193 (given a fixed number of contact tracers), the delay between symptom onset and the  
194 start of tracing,  $1/\tau_{ms}$ , (including getting tested and receiving result), and the fraction of  
195 symptomatic cases that get traced (Figs 1-3).

196



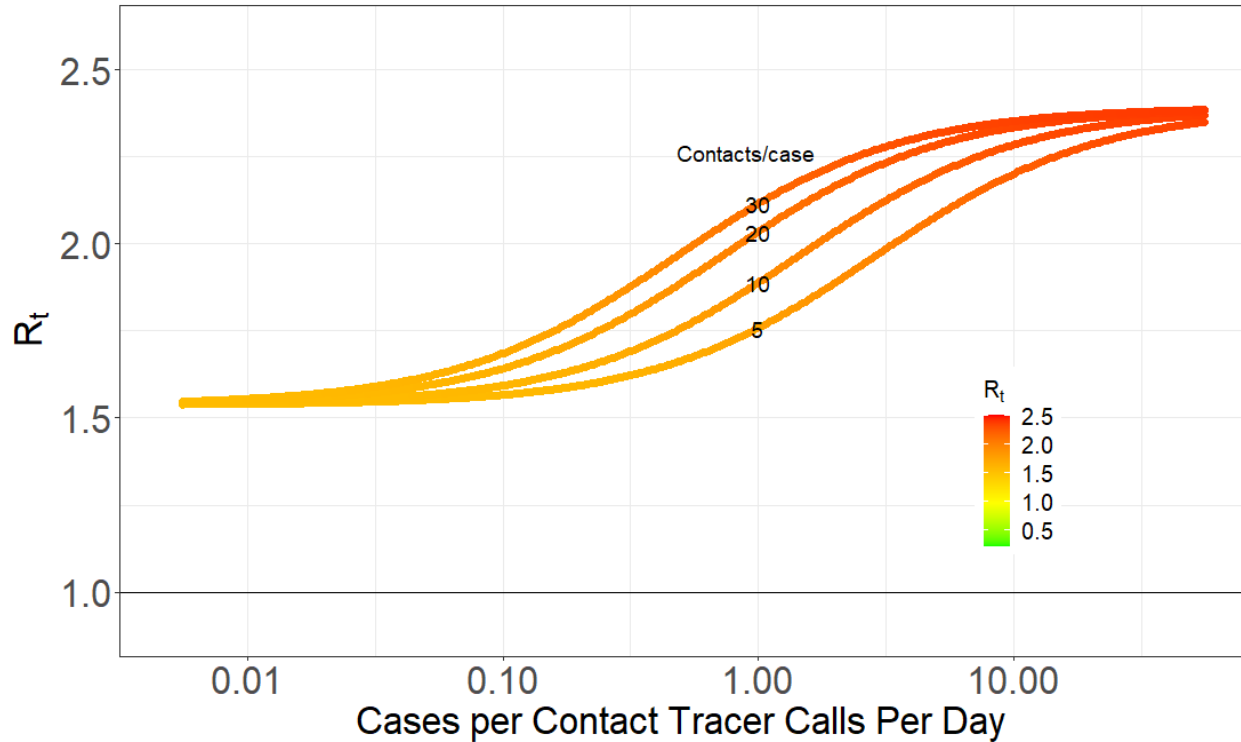
197

198 **Figure 1. Pathogen reproductive ratio  $R_t$  plotted against the number of new cases**  
199 **per contact tracer calls per day for 1-5 day delays ( $1/\tau_{ms}$ ) between symptom onset**  
200 **and the start of contact tracing (including getting tested and receiving result), 10**  
201 **contacts per case (so the average number of contacts each tracer has to reach**  
202 **each day is 10x the x-axis values). With no contact tracing  $R_t$  increases from 2.03**  
203 **to 2.37 as the delay  $1/\tau_{ms}$  increases from 1 to 5 days, which is evident in the y-axis**  
204 **difference between curves in the upper right of the graph where new case**  
205 **burdens are so high contact tracing is ineffective. Delays are indicated by the**  
206 **small numbers on each curve in the left of the plot.**



207  
208  
209  
210  
211  
212  
213  
214  
215  
216  
217  
218  
219  
220  
221  
222  
223  
224

First, the relationship between  $R_0$  and the number of cases per contact tracer calls per day was sigmoid (Figs 1-3); at both high and low numbers adding or removing contact tracers had smaller effects whereas at intermediate case numbers relative to capacity shifting contact tracers would have a larger impact. When the number of new daily cases per contact tracer call per day was high (i.e.  $>1$  or 10 contacts per contact tracer calls per day), contact tracing had relatively little effect in reducing  $R_0$  no matter how long the delay was between symptom onset and the start of tracing,  $1/\tau_{ms}$  (right side of Figs 1; also evident in Figs 2, 3). This is because contact tracing calls took too long, on average ( $>10$  days), to reduce the infectious period of contacts. Note that for the parameter estimates used (Table 1), an average case becomes infectious starting 3.2 days after infection, and is highly or moderately infectious for an average of 7.3 more days ( $\sigma_{ps}$  and  $\sigma_{ms}$ ; Table 1). The exponentially distributed durations for the latent and infectious periods implied by standard compartmental models result in only 37% of individuals leaving each class after the average duration, which results in a relatively smaller benefit of contact tracing beyond this case burden, and resultant delay in reaching contacts of cases.



225

226 **Figure 2. Pathogen reproductive ratio  $R_t$  plotted against the number of Cases per**  
227 **contact tracer calls per day for four different number of contacts per case (5, 10,**  
228 **20, 30; indicated by the small numbers on each curve in the middle of the plot),**  
229 **and an average delay  $1/\tau_{ms}$  of 5 days between symptom onset and contact tracing**  
230 **(including getting tested and receiving result). With no contact tracing  $R_t = 2.39$ .**

231

232 Contact tracers in regions with very high new case numbers relative to contact  
233 tracing capacity ( $>1$  on Fig. 1) would have a larger reduction on  $R_t$  if they were tracing  
234 calls with intermediate numbers of cases (0.02 to 1 cases/contact tracer calls per day).  
235 However, it is worth noting that reducing  $R_t$  is not the same as preventing new cases  
236 (see Discussion below). Nonetheless, if the goal is to reduce  $R_t < 1$  to stop the growth in  
237 cases, the analyses in Figs 1-3 suggest that when new case burdens are high relative  
238 to capacity, population-wide interventions (e.g. social distancing or different levels of  
239 shelter-in-place orders which reduce contact rates,  $\beta$  or  $\kappa$ , and shift the entire curves in  
240 Fig 1-3 downward proportionately; Fig. S2), or orders of magnitude increases in contact  
241 tracing capacity will be needed until  $R_t$  can be effectively reduced by contact tracing.

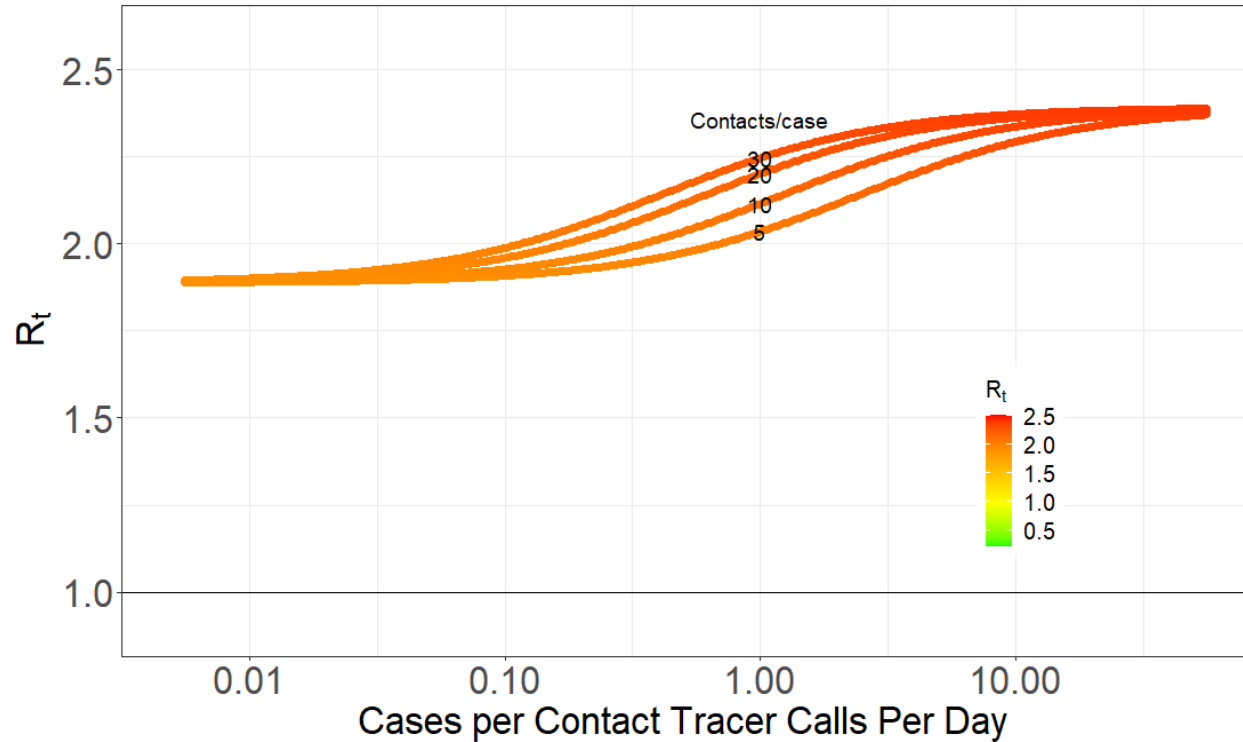
242

When there are few ( $< \sim 0.02$ ) cases per contact tracer call per day, contact

243 tracing was as effective as it could be but excess capacity had little impact, especially  
244 for realistic delays,  $1/\tau_{ms}$ , between symptom onset and the start of tracing (e.g. 3-5  
245 days). Shifting contact tracers to other areas with more cases per contact tracer (0.02 to  
246 0.2) would have minimal impact in increasing  $R_t$  but could help substantially reduce  $R_t$  in  
247 those places with higher new case burdens relative to capacity.

248         Second, increasing delays,  $1/\tau_{ms}$ , between symptom onset and the start of  
249 tracing greatly influenced the efficacy of contact tracing (Fig. 1). With a 5 day delay,  
250 contact tracing could only reduce  $R_0$  by 33% from 2.6 to 1.6 regardless of contact  
251 tracing capacity per case. In contrast, if all symptomatic people sought care and got  
252 tested within 1 day of after symptom onset and results were returned within the next 24  
253 hours ( $1/\tau_{ms} = 2$  days), contact tracing could reduce  $R_0$  by 73% from 2.2 to 0.6. Note  
254 that the effect of delays in increasing  $R_0$  due to delayed removal by testing alone ( $\tau_{ms}$ ) is  
255 small compared to the effect of delays in reducing contact tracing efficiency (Fig 1:  
256 compare differences among curves in upper right of graph where contact tracing is  
257 having little effect to differences among curves in lower left of graph where it has  
258 maximal effect). The number of contacts per case obviously also influences the time  
259 required to trace these contacts (Fig. 2). If allowable (or illegal) gathering sizes  
260 increase, this leads to more contacts per case and a faster decrease in contact tracing  
261 efficacy.

262         Thirdly, if contacts for a substantial fraction of all symptomatic cases do not get  
263 traced and quarantined, T-CT-I/Q is far less effective. Figures 1 and 2 showed an  
264 optimistic scenario where the fraction of symptomatic infections that are tested and  
265 traced is determined only by the delay between symptom onset and testing results  
266 being returned ( $1/\tau_{ms}$ ) (i.e. all symptomatic infections could be tested and traced). With a  
267 5 day delay ( $1/\tau_{ms}=5$ ) (Fig. 2), this results in 38% of infections being detected by testing  
268 in the mildly symptomatic state ( $I_{ms}$ ) which is much higher than estimates of case under-  
269 ascertainment based on seroprevalence studies (25). If only half of these cases are  
270 contact traced ( $f_{tmstr} = 0.5$ ) the maximum impact of contact tracing is smaller: a 21%  
271 reduction in  $R_0$  from 2.39 to 1.89 (Fig 3) rather than a 35% decrease from 2.38 to 1.54  
272 (Fig 2).



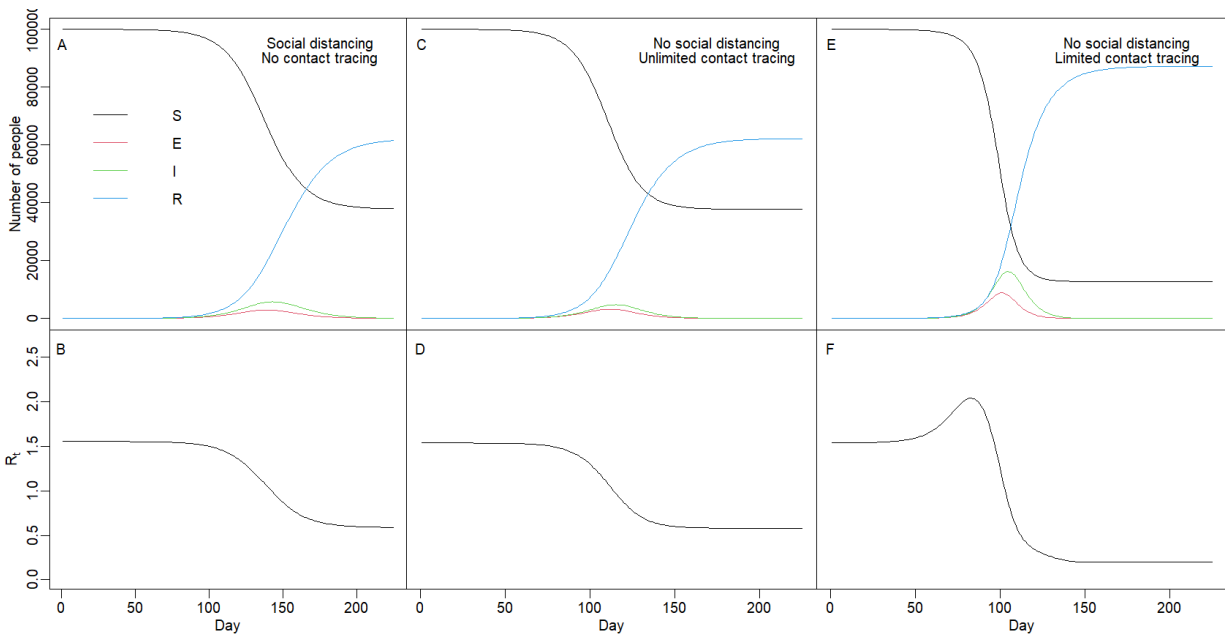
273

274 **Figure 3. Pathogen reproductive ratio  $R_t$  plotted against the number of Cases per**  
275 **contact tracer calls per day for four different number of contacts per case (5, 10,**  
276 **20, 30; indicated by the small numbers on each curve in the middle of the plot), 12**  
277 **calls per contact tracer per day, an average delay  $1/\tau_{ms}$  of 5 days between**  
278 **symptom onset and contact tracing (including getting tested and receiving**  
279 **result). This Figure is the same Figure 2, except only half as many contacts are**  
280 **traced ( $f_{tmstr} = 0.5$ ). With no contact tracing,  $R_t = 2.39$ .**

281

282 Reduced contact tracing efficiency with increasing cases can result in a transient  
283 accelerating epidemic where  $R_t$  increases over time (Fig 4). If contact tracing capacity is  
284 insufficient to quickly trace contacts, then a decrease in contact tracing efficiency can  
285 initially outweigh the depletion of susceptible individuals and lead to an increase in  $R_t$   
286 over time until depletion of susceptibles overwhelms this effect (Fig 4: compare  
287 rightmost panels with limited contact tracing to leftmost panels where social distancing  
288 reduces  $R_t$  to the same initial value as contact tracing). With unlimited contact tracing  
289 this phenomenon does not arise (Fig 4: compare middle panels with unlimited contact  
290 tracing to leftmost panels).

291



292

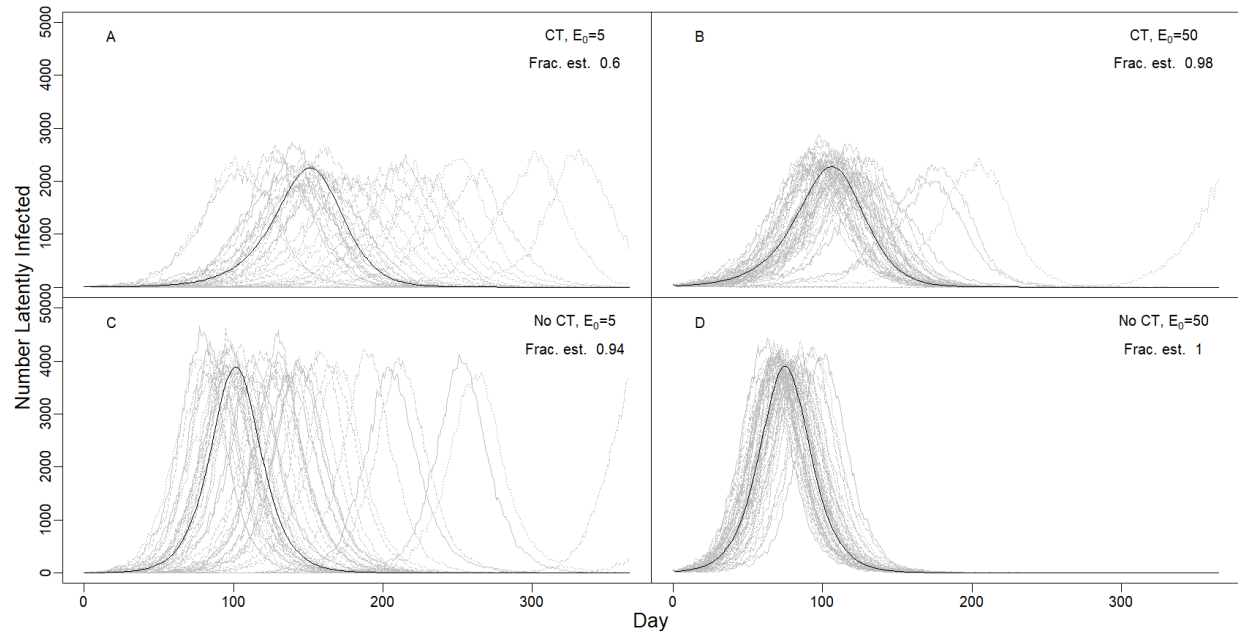
293 **Figure 4. Impact of reduced contact tracing efficiency with increasing cases. Left**  
294 **panels show (A) the number of susceptible, exposed, infected, and recovered**  
295 **individuals and (B) reproductive number,  $R_t$ , over time with no contact tracing but**  
296 **social distancing ( $\kappa = 0.65$ ) set to give same initial  $R_0$  (1.55) as with contact**  
297 **tracing. Middle panels (C, D) show the same variables with unlimited contact**  
298 **tracing (1500 contact tracers making 12 calls/day; 15 contacts per case;  $1/\tau_{ms} =$**   
299 **5d;  $f_{tmstr} = 1$ ) but no social distancing ( $\kappa = 1$ ). Right panels (E, F) show the same**  
300 **variables and parameters as (C, D) but with limited contact tracing (5 contact**  
301 **tracers).**

302

303 The impact of contact tracing in reducing the pathogen reproductive number  $R_t$   
304 has two consequences on the temporal timing and establishment of epidemics. First, as  
305 is well known, reducing  $R_t$  delays and reduces the peak of the epidemic (Fig 5 top vs  
306 bottom panels). Second, and less appreciated, stochastic variation in  $R_t$  can lead to very  
307 different timing of epidemics if the initial number of infected individuals is low (Fig 5 left  
308 panels), and variation is larger if  $R_t$  is lower (Fig 5A vs Fig 5C). Finally, heterogeneity in  
309 individual transmission can result in local fadeout of the pathogen and this is more if  
310 contact tracing reduces  $R_t$  so that it is closer to 1, and if the number of infected

311 individuals is lower.

312



313

314 **Figure 5. Variability in the timing and outcome of epidemics due to stochastic**  
315 **variation in individual  $R_t$ . Lines show number of latently infected individuals (in**  
316 **the E class) over time for 1 year with moderate social distancing that reduces**  
317 **contact rates by 30% ( $\kappa = 0.7$ ). Grey lines show a single stochastic simulation and**  
318 **the black line shows the deterministic outcome. Frac. est. is the fraction of**  
319 **epidemics that establish (i.e. the maximum number of infected at any time**  
320 **exceeds the starting number infected). Four scenarios include different starting**  
321 **numbers of latently infected individuals on day 0,  $E_0$  (A, C: 5; B, D: 50), and with**  
322 **(A, B) or without (C, D) contact tracing (CT) which lowered  $R_0$  from 1.67 to 1.32.**  
323 **The delay from symptom onset to testing and tracing was 5d, but only half of**  
324 **cases were traced ( $f_{tmstr} = 0.5$ ), as in Fig 3. The modeled population of 100,000**  
325 **people had 15 tracers making 12 calls/day, and each case had an average of 15**  
326 **contacts which is intermediate between pre-lockdown and lockdown conditions.**

327

328

## 329 Discussion

330

The two main strategies that have been used to control COVID-19 are T-CT-I/Q

331 and society-wide social distancing interventions (including closing businesses, banning  
332 gatherings, wearing masks, etc.) (9). Closing businesses has had devastating impacts  
333 on employment and economies, as well as cascading impacts on society. T-CT-I/Q has  
334 far smaller economic and societal costs, but its efficacy in controlling epidemics is not  
335 fully understood, and some studies suggest that it is insufficient to keep  $R_t$  below 1 in  
336 many settings, especially without digital contact tracing (10, 11, 18). We examined how  
337 the efficacy of contact tracing decreases with increasing case burden. At high case  
338 burdens relative to contact tracing capacity, contact tracing reached most contacts too  
339 late and had little effect on  $R_t$ . Conversely when case numbers were very low relative to  
340 contact tracing capacity, there was excess capacity and, all else being equal, contact  
341 tracers could be used more effectively in higher case burden settings with very small  
342 impacts on local transmission. We note that the exact number of contact tracers needed  
343 to reduce  $R_t$  depends on the number of contacts per case and the number of calls each  
344 tracer can make each day (Fig 2). However, the key quantity appears as a ratio of case-  
345 contacts per contact tracer calls per day. Thus, each contact tracing team (e.g. a US  
346 County) can use local estimates of contacts per case and the number of calls each  
347 tracer can make each day to determine where they are on the modelled relationships  
348 (Figs 1-3).

349 A major caveat must be kept in mind in interpreting these results. A smaller  
350 reduction in  $R_t$  (e.g. 10%) in one population can prevent more infections (especially over  
351 multiple generations of transmission) than a larger (e.g. 20%) reduction in  $R_t$  in a  
352 second population if  $R_t$  in the second location is lower (especially when  $R_t > 1$  in the first  
353 population), or when there is a larger number of infected individuals in the first  
354 population. Thus, transferring contact tracers from a region with a high case burden  
355 relative to contact tracing capacity to maximize their efficacy in reducing  $R_t$  should only  
356 be done if other measures (e.g. social distancing) will be put into place to reduce  $R_t$   
357 where case numbers are high. More generally, allocation of contact tracers to maximize  
358 the number of cases prevented given an array of tools would require a complex  
359 dynamic analysis beyond that examined here.

360 We also found that the efficacy of contact tracing itself, regardless of capacity,  
361 was strongly influenced by delays between the onset of symptoms and the beginning of

362 tracing, as well as the fraction of symptomatic infections that were traced. Unless delays  
363 were short and the fraction of symptomatic cases that were traced was high, contact  
364 tracing had limited effects in reducing  $R_t$ . This finding parallels results from other studies  
365 demonstrating the large effects of delays in reducing efficacy of isolating infections by  
366 testing alone (26). We note that in the model considered here, only symptomatic  
367 individuals were removed by testing (pre-symptomatic and asymptomatic infections  
368 were not tested) which leads to a much smaller impact of testing on  $R_t$ . Our results  
369 emphasize the importance of encouraging people to get tested as soon as possible  
370 after mild symptom onset, and having sufficient testing capacity to return their results  
371 quickly. Similarly, the fraction of symptomatic infections that get tested and traced is  
372 poorly known, but if the ratio of infections to cases from seroprevalence studies in some  
373 locations is approximately correct (e.g. 10:1; (25)), then contact tracing will have very  
374 limited effects in reducing transmission.

375 Allocation of contact tracing resources can be most efficiently deployed in two  
376 ways. First, contact tracing is much more effective when infections are detected soon  
377 after symptom onset. One should prioritize these individual cases for tracing since their  
378 contacts are likely to be earlier in their infections and quarantining them will cut off most  
379 or all of their infectious period. If one knows the date of contact between the case and  
380 the contact, one could also prioritize tracing more recent contacts and those that had  
381 contact with the case during the case's days of peak infectiousness just before and after  
382 symptom onset (27, 28). Second, if one is attempting to limit transmission in multiple  
383 regions (e.g. US counties within a state) one could deploy contact tracers to counties  
384 where they will be able to have the most impact: from places with excess capacity to  
385 those with intermediate numbers of cases per contact tracer calls per day. Conversely,  
386 if contact tracers cannot quarantine the contacts of cases within 10-12 days of the  
387 case's symptom onset, they will be unlikely to effectively reduce transmission from  
388 those contacts.

389 Our results also offer insight on two phenomena observed in COVID-19  
390 epidemics that are not fully understood. First, epidemic dynamics sometimes differ  
391 enormously between places that seem otherwise similar. This may be due to  
392 differences in social behavior or contact patterns, but our results illustrate that



393 stochastic chance may also play a role in shifting the timing of epidemics by more than  
394 a month, especially when the initial number of cases is low and  $R_t$  is closer to 1 (i.e.  
395 when lockdowns are first lifted) so that populations spend longer periods of time with  
396 few cases where stochastic variation is most important. Second, staged business re-  
397 openings have sometimes led to accelerating or runaway epidemics. These may be due  
398 to sudden changes in social behavior, but decreases in contact tracing efficiency may  
399 also contribute to these accelerating epidemics, if contact tracing was playing a  
400 significant role in limiting transmission. Increasing contact tracing capacity could limit  
401 this epidemic acceleration as cases increase, which suggests that training a reserve  
402 capacity of tracers to be used following case surges or being able to deploy a mobile  
403 tracing force could help limit runaway epidemics.

404 More broadly, contact tracing could play an important role in limiting transmission  
405 of SARS-CoV-2 and other pathogens. However, we found that its efficacy depends on  
406 participation in seeking testing immediately following symptom onset and quick return of  
407 test results, as well as sufficient contact tracing capacity if case numbers surge.  
408 Shortcomings in each of these factors greatly limit its efficacy, which could lead to  
409 implementation of much more damaging measures to control transmission, including  
410 widespread business and school closures. Investments in public health, including  
411 testing, contact tracing, and public outreach to encourage health seeking when  
412 symptomatic, is likely a much more cost-effective approach to control COVID-19.

413

414 **Acknowledgements:** We thank the dozens of scientists and public health practitioners  
415 who have informed this work through comments and discussions.

416

#### 417 **Literature Cited**

- 418 1. J. T. Wu, K. Leung, G. M. Leung, Nowcasting and forecasting the potential domestic and  
419 international spread of the 2019-nCoV outbreak originating in Wuhan, China: a  
420 modelling study. *Lancet* **395**, 689-697 (2020).
- 421 2. A. Remuzzi, G. Remuzzi, COVID-19 and Italy: what next? *Lancet* **395**, 1225-1228  
422 (2020).
- 423 3. P. Zhou *et al.*, A pneumonia outbreak associated with a new coronavirus of probable bat  
424 origin. *Nature* **579**, 270-+ (2020).
- 425 4. N. Zhu *et al.*, A Novel Coronavirus from Patients with Pneumonia in China, 2019. *N.*  
426 *Engl. J. Med.* **382**, 727-733 (2020).

- 427 5. S. Flaxman *et al.*, Estimating the effects of non-pharmaceutical interventions on COVID-  
428 19 in Europe. *Nature* 10.1038/s41586-020-2405-7, 15.
- 429 6. Y. X. Ng *et al.*, Evaluation of the Effectiveness of Surveillance and Containment  
430 Measures for the First 100 Patients with COVID-19 in Singapore - January 2-February  
431 29, 2020. *MMWR-Morb. Mortal. Wkly. Rep.* **69**, 307-311 (2020).
- 432 7. R. Pung *et al.*, Investigation of three clusters of COVID-19 in Singapore: implications for  
433 surveillance and response measures. *Lancet* **395**, 1039-1046 (2020).
- 434 8. J. R. Koo *et al.*, Interventions to mitigate early spread of SARS-CoV-2 in Singapore: a  
435 modelling study. *Lancet Infect. Dis.* **20**, 678–688 (2020).
- 436 9. B. J. Cowling, A. E. Aiello, Public Health Measures to Slow Community Spread of  
437 Coronavirus Disease 2019. *J. Infect. Dis.* **221**, 1749-1751 (2020).
- 438 10. B. J. Cowling *et al.*, Impact assessment of non-pharmaceutical interventions against  
439 coronavirus disease 2019 and influenza in Hong Kong: an observational study. *Lancet*  
440 *Public Health* **5**, E279-E288 (2020).
- 441 11. J. Hellewell *et al.*, Feasibility of controlling COVID-19 outbreaks by isolation of cases and  
442 contacts. *Lancet Global Health* **8**, E488-E496 (2020).
- 443 12. J. A. Firth *et al.*, Using a real-world network to model localized COVID-19 control  
444 strategies. *Nat. Med.* 10.1038/s41591-020-1036-8.
- 445 13. G. Giordano *et al.*, Modelling the COVID-19 epidemic and implementation of population-  
446 wide interventions in Italy. *Nat. Med.* 10.1038/s41591-020-0883-7.
- 447 14. S. Marcel *et al.*, COVID-19 epidemic in Switzerland: on the importance of testing,  
448 contact tracing and isolation. *Swiss Medical Weekly* **150** (2020).
- 449 15. S. M. Moghadas *et al.*, The implications of silent transmission for the control of COVID-  
450 19 outbreaks. *Proc. Natl. Acad. Sci. U. S. A.* **117**, 17513-17515 (2020).
- 451 16. C. N. Ngonghala *et al.*, Mathematical assessment of the impact of non-pharmaceutical  
452 interventions on curtailing the 2019 novel Coronavirus. *Math. Biosci.* **325** (2020).
- 453 17. R. P. Walensky, C. del Rio, From Mitigation to Containment of the COVID-19 Pandemic  
454 Putting the SARS-CoV-2 Genie Back in the Bottle. *JAMA-J. Am. Med. Assoc.* **323**, 1889-  
455 1890 (2020).
- 456 18. L. Ferretti *et al.*, Quantifying SARS-CoV-2 transmission suggests epidemic control with  
457 digital contact tracing. *Science* **368**, 619-+ (2020).
- 458 19. F. Zhou *et al.*, Clinical course and risk factors for mortality of adult inpatients with  
459 COVID-19 in Wuhan, China: a retrospective cohort study. *Lancet* **395**, 1054-1062  
460 (2020).
- 461 20. J. A. Lewnard *et al.*, Incidence, clinical outcomes, and transmission dynamics of severe  
462 coronavirus disease 2019 in California and Washington: prospective cohort study. *BMJ-  
463 British Medical Journal* **369**, 10 (2020).
- 464 21. O. Diekmann, J. A. P. Heesterbeek, M. G. Roberts, The construction of next-generation  
465 matrices for compartmental epidemic models. *J. R. Soc. Interface* **7**, 873-885 (2010).
- 466 22. B. M. Althouse *et al.*, Stochasticity and heterogeneity in the transmission dynamics of  
467 SARS-CoV-2. *arXiv arXiv:2005.13689*, <https://arxiv.org/abs/2005.13689> (2020).
- 468 23. A. Endo, Centre for the Mathematical Modelling of Infectious Diseases COVID-19  
469 Working Group, S. Abbott, A. J. Kucharski, S. Funk, Estimating the overdispersion in  
470 COVID-19 transmission using outbreak sizes outside China. *Wellcome Open Research*  
471 **5**, <https://doi.org/10.12688/wellcomeopenres.15842.12681> (2020).
- 472 24. D. C. Adam *et al.*, Clustering and superspreading potential of SARS-CoV-2 infections in  
473 Hong Kong. *Nat. Med.* 10.1038/s41591-020-1092-0, 10.1038/s41591-41020-41092-  
474 41590 (2020).
- 475 25. E. S. Rosenberg *et al.*, Cumulative incidence and diagnosis of SARS-CoV-2 infection in  
476 New York,. *Ann. Epidemiol.* **48**, 23-29 (2020).

- 477 26. D. B. Larremore *et al.*, Surveillance testing of SARS-CoV-2. *medRxiv*,  
478 doi.org/10.1101/2020.1106.1122.20136309 (2020).
- 479 27. A. M. Wilson *et al.*, Quantifying SARS-CoV-2 infection risk within the Apple/Google  
480 exposure notification framework to inform quarantine recommendations. *medRxiv*  
481 10.1101/2020.07.17.20156539 (2020).
- 482 28. X. He *et al.*, Temporal dynamics in viral shedding and transmissibility of COVID-19. *Nat.*  
483 *Med.* **26**, 672-+ (2020).
- 484 29. S. Abbott *et al.*, Estimating the time-varying reproduction number of SARS-CoV-2 using  
485 national and subnational case counts [version 1; peer review: awaiting peer review].  
486 *Wellcome Open Research* **5**, 112 (2020).
- 487 30. R. Verity *et al.*, Estimates of the severity of coronavirus disease 2019: a model-based  
488 analysis. *Lancet Infect. Dis.* **20**, 669-677 (2020).
- 489 31. T. W. Russell *et al.*, Estimating the infection and case fatality ratio for coronavirus  
490 disease (COVID-19) using age-adjusted data from the outbreak on the Diamond  
491 Princess cruise ship, February 2020. *Eurosurv.* **25**, 12 (2020).
- 492 32. D. C. Buitrago-Garcia *et al.*, Asymptomatic SARS-CoV-2 infections: a living systematic  
493 review and meta-analysis. *medRxiv* 10.1101/2020.04.25.20079103 (2020).
- 494 33. M. Cevik *et al.*, SARS-CoV-2, SARS-CoV-1 and MERS-CoV viral load dynamics,  
495 duration of viral shedding and infectiousness: a living systematic review and meta-  
496 analysis. *medRxiv* 10.1101/2020.07.25.20162107 (2020).
- 497
- 498
- 499

500 **Tables**

501 **Table 1. Parameter values for the model. All rates are in days<sup>-1</sup> and many are**  
 502 **based on the inverse of measured durations.**

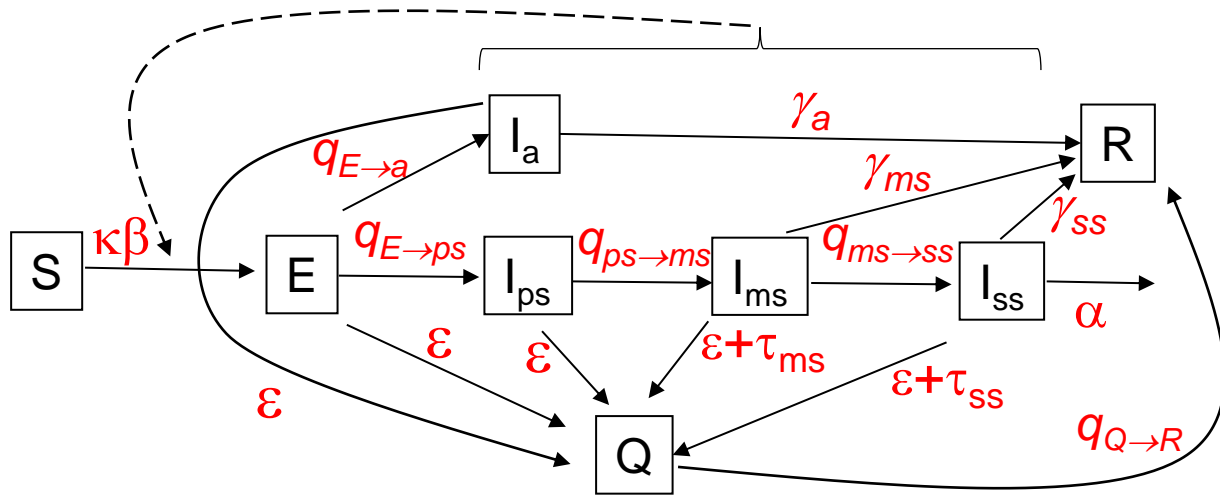
| Parameter               | Value or range | Description   | Reference or Derivation  |
|-------------------------|----------------|---|--|
| $\tau_{ms}$             | 0.2-1          | Testing removal rate for $I_{ms}$ (1/delay from onset to testing & tracing)         | Scenarios explored   |
| $\beta$                 | 0.37           | Contact rate  | Set to give plausible pre-lockdown $R_0 \cong 2-3$ (29)  |
| $f_{tmstr}$             | 0.5 or 1       | Fraction of mildly symptomatic cases detected by testing whose contacts were traced | Scenarios explored   |
| $\kappa$                | 0-1            | Social distancing factor  | Adjusted to produce $R_t \cong 1.2-1.7$ ; consistent with data post-lockdown; (29)   |
| $\alpha$                | 0.0025         | Disease caused death rate   | estimated from IFR* ( $\gamma_{ms} + \gamma_{ss} + q_{E \rightarrow a}$ )/(1-IFR) = using infection fatality ratio IFR = 0.0066; (30, 31)        |
| $q_{E \rightarrow a}$   | 0.078          | Transition rate exposed to asymptotically infected                                  | Estimated from $q_{E \rightarrow a} = f_{asymp}(q_{E \rightarrow ps}) / (1 - f_{asymp})$ using fraction asymptomatic ( $f_{asymp} = 0.2$ ); (32) |
| $q_{E \rightarrow ps}$  | 1/3.2          | 1/(duration latent period)  | (28)   |
| $q_{ps \rightarrow ms}$ | 1/2.3          | 1/(duration pre-symptomatic period)   | (28)   |
| $q_{ms \rightarrow ss}$ | 1/8            | 1/duration mild symptoms  | (19, 20)   |
| $\gamma_a$              | 1/8            | Asymptomatic recovery rate  | Based on average ratio of shedding durations compared to symptomatic cases (33)  |
| $\gamma_{ms}$           | 1/5,           | Mild infection recovery rate  | (28)   |
| $\gamma_{ss}$           | 1/10.7         | Severe symptom recovery rate  | (20)   |
| $\gamma_Q$              | 1/14           | Quarantined recover rate  | Does not affect dynamics   |
| $\sigma_a$              | 1              | Relative infectiousness   | (33)   |

|               |       |  |                   |
|---------------|-------|--|-------------------|
|               |       | asymptomatic:mildly symptomatic                            |                   |
| $\sigma_{ps}$ | 1.81  | Relative infectiousness pre-symptomatic:mildly symptomatic | (28)              |
| $\sigma_{ms}$ | 1     | Relative infectiousness                                    | (reference level) |
| $\sigma_{ss}$ | 0.008 | Relative infectiousness severe symptoms:mildly symptomatic | (28)              |

503

504

505

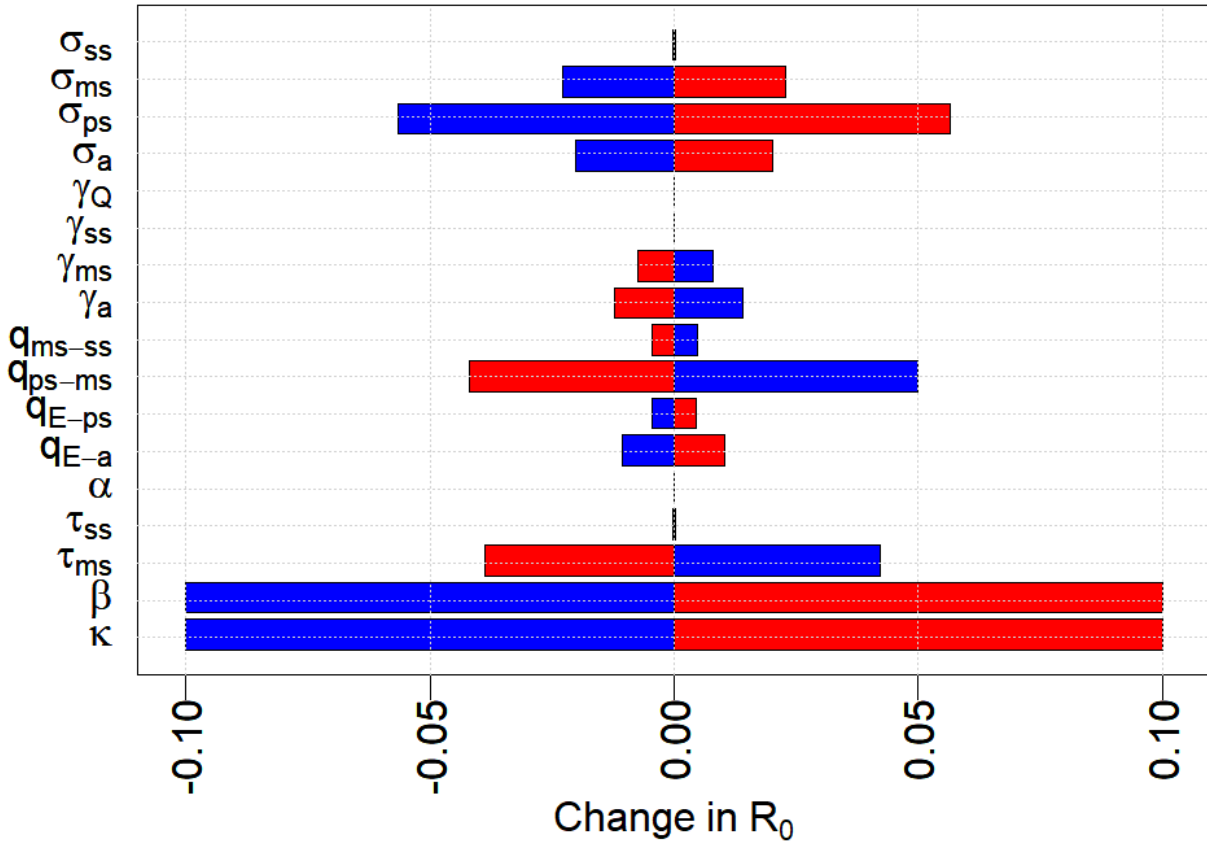


506

507 **Figure S1. Compartmental model of SARS-CoV-2. See text for equations and**  
 508 **parameter values. Boxes represent Susceptible (S), Exposed (E), Infected (I),**  
 509 **recovered (R), and Quarantined (Q) classes. There are four compartments for**  
 510 **infected individuals that reflect symptom severity (asymptomatic,  $I_a$ , pre-**  
 511 **symptomatic,  $I_{ps}$ , mildly symptomatic,  $I_{ms}$ , and severely symptomatic,  $I_{ss}$ ).  $\kappa$  is a**  
 512 **social distancing factor between 0 and 1 that modifies the contact rate  $\beta$ ,  $\sigma$  are**  
 513 **infectiousness for each of the I classes,  $q$  are transition rates between classes**  
 514 **given by the subscripts separated by the arrow ( $q_{E \rightarrow ps}$  is the transition rate**  
 515 **between the E and  $I_{ps}$  classes),  $\varepsilon$  is the rate of removal by contact tracing from the**  
 516 **E or I classes to the quarantined class Q,  $\tau$  are the removal rate by testing of**  
 517 **mildly symptomatic or severely symptomatic infected individuals,  $\alpha$  is the**  
 518 **disease-caused death rate, and  $\gamma$  are the recovery rates to the R class. The**  
 519 **dashed line and bracket indicate that all 4 classes of infected individuals**  
 520 **contribute to transmission.**

521

522



523

524 **Figure S2. Sensitivity analysis.** The plot shows how much  $R_0$  changes from a ten  
525 percent increase (red) or ten percent decrease (blue) in that model parameter  
526 relative to values in Table 1 (with  $\tau_{ms} = 0.2$ ;  $f_{tmstr} = 1$ ;  $\kappa = 1$ ).  $R_t$  scales linearly with  $\beta$   
527 and  $\kappa$ , whereas  $q_{ps \rightarrow ms}$ ,  $\tau_{ms}$ , and  $\sigma_{ps}$  have half as large an effect as  $\beta$  or  $\kappa$  and other  
528 parameters are even less influential.

529